Dynamical Effects in the Interaction of Ion Beams with Solids

Ryan Hatcher,[1] Matthew Beck,[1] Alan Tackett,[1] and Sokrates T. Pantelides[1,2]
[1]*Department of Physics and Astronomy, Vanderbilt University, Nashville, Tennessee 37235, USA*
[2]*Oak Ridge National Laboratory, Oak Ridge, Tennessee 37831, USA*
(Received 8 May 2007; published 13 March 2008)

Calculations of the stopping power (SP) of ion beams in solids have been based on a homogeneous electron gas scattering off a static atom and entail at least one free parameter. Here we report *dynamical* simulations of ions channeled in silicon. Time-dependent density-functional theory (TDDFT) is used. The calculated SPs are in excellent agreement with the observed oscillatory dependence on atomic number. TDDFT calculations for a homogeneous electron gas demonstrate that both dynamical response and nonuniformities in the electron density are essential to reproduce the data without free parameters.

DOI: 10.1103/PhysRevLett.100.103201 PACS numbers: 34.50.Bw, 31.15.ee, 61.85.+p

The dynamics of energetic ion beams traversing solids and the resulting ion-to-solid energy transfer are widely studied. Stopping power (SP) [1] is a key measurable quantity that characterizes this energy transfer and has served as a critical test of theories for the underlying mechanisms. Early theoretical work on SP was motivated by the stopping of elementary particles in solids [2,3]. Since the 1960s ion beams have been used and studied extensively in the context of materials processing. The dynamics of well-channeled ion beams in semiconductors [4–7] have become an important test for theoretical models of SP (see [8], and references therein). Well-channeled ions represent a limiting case for ion-solid interactions in which projectile ions essentially lose energy only to the crystal valence electrons. Even so, SP exhibits an oscillatory behavior as a function of projectile atomic number Z. At high projectile ion velocities, where available theories best predict observed behavior, these so-called Z_1 oscillations damp out.

Theories of SP in the low-velocity regime have been based on the assumption that the electrons in the solid can be approximated by a homogeneous electron gas (HEG). Several authors have calculated SP's, using linear-response theory [9–13]. Other authors have used scattering theory in the projectile ion's reference frame: the electrons in the target material are scattered by the potential of the static ion [1,14,15]. The SP is then determined from the phase shifts of this potential. The electron density of the HEG employed has been obtained from model calculations [16] or fits to measured data [15]. The results of such theories reproduce the observed oscillations at least qualitatively. In the one-parameter theory of Echenique *et al.* [15] for $\langle 110 \rangle$ Si channels and ions with $Z_1 = 5$–19, the calculated SPs are in good agreement with the data except for the large-Z ions ($Z_1 = 15$–19).

Despite the apparent success of these theories, serious questions remain open about their key assumptions. The electron density in semiconductor channels is not uniform. In the Si $\langle 110 \rangle$ channel, it varies by more than an order of magnitude in the region traversed by the ion. Penalba *et al.* [17] extended the approach described above to include inhomogeneities in the target by averaging over the densities in the channel, which led to better agreement with experiment over the entire range of Z_1. In addition, since the ion's velocity is comparable to those of the crystal's valence electrons, calculating the scattering potential by keeping the ion's electrons in their ground-state configuration is a highly limiting approximation. In this Letter we report results of fully dynamical, parameter-free calculations of the SP for 15 projectile ions traversing the $\langle 110 \rangle$ and $\langle 111 \rangle$ channels in a Si crystal. The calculations were performed using time-dependent density-functional theory (TDDFT) [18]. The calculated SPs are in excellent quantitative agreement with the observed Z_1 oscillations. Transitory bonds are observed between the projectile and crystal atoms, but have no net effect on the SP. We find that both the dynamical response and the inhomogeneities in the solid's electron distribution play major roles in determining SP. We probed these roles by performing TDDFT calculations for the same 15 projectile ions traversing a HEG. We show that when the electron density is treated as uniform, the agreement between theory and experiment is substantially worse for SPs calculated using a fully dynamical model than those obtained from previous static calculations.

In the present calculations, the initial system, consisting of a perfect silicon crystal and physically separated free atom, are described with density-functional theory (DFT), the local density approximation (LDA) for exchange correlation, pseudopotentials, and plane waves. At time $t = t_0$ the free atom is given an initial velocity and aimed down the center of a $\langle 110 \rangle$ or $\langle 111 \rangle$ channel in a Si film. As the system evolves in time, the electronic wave functions propagate by applying the time-evolution operator

$$\psi(t) = \hat{U}(t_0, t)\psi(t_0), \tag{1}$$

where

$$\hat{U}(t_0, t) = \mathcal{T} \exp\left[-\frac{i}{\hbar} \int_{t_0}^{t} dt' \, \hat{H}(t') \right]. \quad (2)$$

Here $\mathcal{T}$ is the time-ordering operator and $\hat{H}$ is the time-dependent Kohn-Sham Hamiltonian with the adiabatic LDA exchange-correlation potential [19].

The time-ordered evolution operator in Eq. (2) can be written as an infinite product:

$$\hat{U}(t_0, t) = \hat{U}(t_{N-1}, t_N) \ldots \hat{U}(t_1, t_2) \hat{U}(t_0, t_1) = \lim_{\substack{\Delta \to 0 \\ N \to \infty}} \prod_{n=0}^{N-1} \hat{U}(t_n, t_{n+1}). \quad (3)$$

Here we have defined $t_n \equiv t_0 + n\Delta$. In the limit as the time step becomes vanishingly small, $\Delta \to 0$, the time-evolution operator Eq. (2) becomes

$$\lim_{\Delta \to 0} \hat{U}(t_n, t_n + \Delta) = e^{-(i/\hbar)\Delta \hat{H}(t_n)}. \quad (4)$$

Thus, applying the time-evolution operator numerically requires that Δ be small enough that the Hamiltonian does not change appreciably during a *single* time step. The Chebychev expansion [20] is used to expand the exponential operator in Eq. (4).

The total energy of the electron-ion system can be written as the sum of the kinetic energy of the nuclei and the instantaneous energy [21]

$$E_{\text{tot}} = E_{\text{nuc}} + E_{\text{instant}}, \quad (5)$$

where E_{instant} is defined as the Kohn-Sham total energy calculated from the (fully time-dependent and time-evolved) wave functions and nuclear positions at each time step. E_{tot} is conserved in the absence of external interactions such as photoemission or photoabsorption [21], which are not permitted in the present method. Therefore the conservation of E_{tot} is a test of numerical stability in the present method. The forces on the ions are calculated using the Hellmann-Feynman theorem and the ions are time stepped via Newton's second law.

Our implementation of TDDFT was built on the SOCORRO code [22]. In order to assess the new code and test Eq. (5), we simulated a binary scattering event between two Si atoms in vacuum. A "target" atom initially at rest was placed at the center of the calculation cell. A projectile Si atom with a velocity of 2.11 Å/fs (6.52 keV) was set on a trajectory past the target atom with an impact parameter of 1.0 Å. The atom velocities evolve during the simulation. The quantities E_{nuc} and E_{instant} were monitored as a function of simulation time (equivalently, as a function of the position of the projectile atom) for both a TDDFT calculation and Born-Oppenheimer molecular dynamics (BOMD), also known as Car-Parrinello dynamics. In BOMD the electrons are always in their instantaneous ground state as the nuclei are time stepped. A comparison of the results is presented in Fig. 1. In the TDDFT calculation, 12.1 eV is transferred to the electron system as the projectile atom scatters from the target atom. In the BOMD calculation, no net energy is retained by the electrons after the scattering event, because the instantaneous energy of the electrons is, by definition, the ground-state energy of the system, and is therefore a function only of the interatomic distance. The transfer of energy captured in the TDDFT calculation demonstrates that this TDDFT formulation is suitable for SP calculations. The figure also demonstrates that $\Delta E_{\text{nuc}}(t) = -\Delta E_{\text{instant}}(t)$, verifying that the total energy of the system defined by Eq. (5) remains constant throughout.

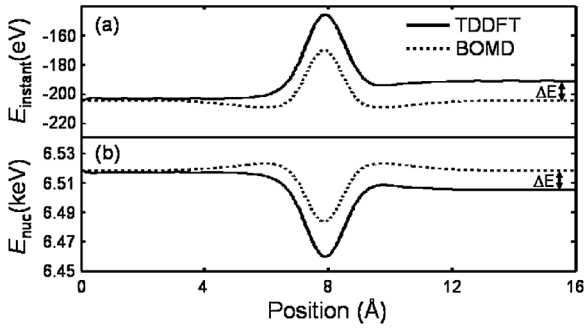

FIG. 1. (a) Instantaneous DFT energies and (b) kinetic energy of the nuclei from TDDFT and BOMD simulations of a binary collision of two atoms. $\Delta E \approx 12.1$ eV is the transfer of energy from the kinetic energy of the nuclei to the electrons in the TDDFT simulation. In the BOMD calculation, there is no net transfer of energy.

We now turn to calculations of SP for ions traversing a Si ⟨110⟩ channel. Figure 2 shows the $21 \times 11 \times 11$ Å^3 calculation cell, containing a bulk terminated, 72 atom, crystalline silicon film. The projectile atom is initially placed in the vacuum region outside the crystal. The ion core that carries the mass of the projectile atom is given an initial velocity $v = 15$ Å/fs perpendicular to the crystal surfaces as in the experiment of Eisen [6]. The valence electrons in the entire system start in their ground state and evolve during the simulation. The time step was $\sim 10^{-3}$ fs, depending on the species of the projectile atom, which tra-

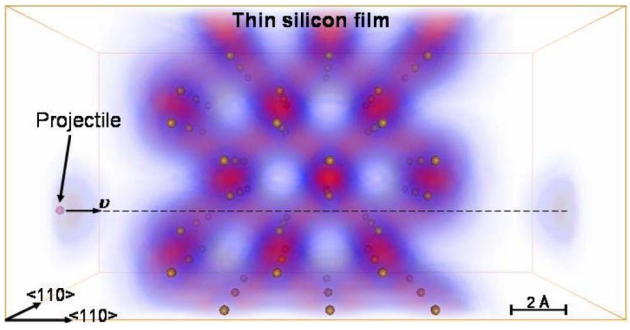

FIG. 2 (color online). Simulation cell for SP calculations. The projectile atom, with initial velocity v, travels through a ⟨110⟩ channel of the crystalline silicon film.

verses the calculation cell in ~1.3 fs. Figure 3 shows the ion kinetic energy, $E_{\mathrm{nuc}}(x)$, as a function of the position of a Mg projectile moving through the calculation cell depicted in Fig. 2. Plots for all considered projectile atoms are qualitatively similar. Once the ion enters the crystal (at ~5 Å in Fig. 3), kinetic energy is lost to the crystal electrons and the SP can be calculated from the overall slope of either $E_{\mathrm{nuc}}(x)$ or $E_{\mathrm{instant}}(x)$.

Oscillating energy transfer between the projectile ion core and valence electrons is observed immediately after the projectile begins moving. The ion core first loses energy to the electrons; the electrons catch up, overshoot, and transfer energy back to the ion core, and so on. To test for any effect of this on SP, we carried out calculations placing the crystalline film at different points of the projectile's in-vacuum trajectory. In Fig. 3, the solid black curve and dashed red curve correspond to projectiles starting 15.9 Å and 8 Å from the film, respectively. The SP for both curves is the same once the projectile is inside the crystal. We also prepared the projectile in various positively charged states and verified that the energy transfer in the crystal (the SP) is independent of initial charge.

The curve shown in the inset in Fig. 3 is the deviation of $E_{\mathrm{nuc}}(x)$ from the straight line fit to $E_{\mathrm{nuc}}(x)$ shown as a dashed line. The six vertical dotted lines in Fig. 3 and the inset indicate the points at which the projectile passes through a perpendicular [110] plane of atoms and has its closest approach with the lattice atoms. The minima of the oscillations in $E_{\mathrm{nuc}}(x)$ shown in the inset of Fig. 3 represent transitory bonds formed between the projectile and lattice atoms in the channel perimeter. Bonds with the nearest neighbors in each passing crystal plane form, then break, and then new bonds form with nearest neighbors in the next crystal plane, as demonstrated in Fig. 4. All projectile atoms showed qualitatively similar behavior. It is clear from Fig. 3 that the formation of transitory bonds is only a small contribution to the overall SP.

The SP calculation described above was repeated for ion species ranging from B ($Z_1 = 5$) to K ($Z_1 = 19$). The calculated SP values are given by the dark blue curve with solid diamonds in Fig. 5. The experimental values reported by Eisen [6] are shown by the solid black points. The overall agreement between theory and data is excellent. Figure 5(a) also shows the theoretical results of Echenique *et al.* [15] (gray curve and points). The method of that paper approximates the crystal with a HEG and keeps the ion in its ground state while crystal electrons scatter from it. In addition, the method entails a free parameter (the constant electron density of the HEG) that was fitted to the experimental SP value of B. As can be seen from Fig. 5(a), the SP values calculated by this method are quite good for projectile species up to Al, but are too small for the heavier projectile species starting with Si ($Z_1 =$ 15–19).

In order to explore the roles of dynamical effects and the nonuniformities in the electron density in the ⟨110⟩ crystal channel, a second set of TDDFT calculations was performed for projectiles moving through a HEG. We set the density of the HEG to $r_s = 2.38$, which was the value adopted by Echenique *et al.* [15] for their calculations at which the TDDFT HEG calculated SP was equal to the experimentally observed SP for B. The results are shown as a dashed blue curve with open diamonds in Fig. 5(a), demonstrating that inclusion of dynamical effects produces substantial changes to the values obtained by Echenique *et al.* and, in fact, makes the overall agreement with the data worse. We also pursued TDDFT/HEG calculations at a different density (2.23), determined to yield the experimental SP value for B. The results are shown in Fig. 5(a). The net conclusion is that dynamical effects are not negligible and that the HEG approximation fails to yield

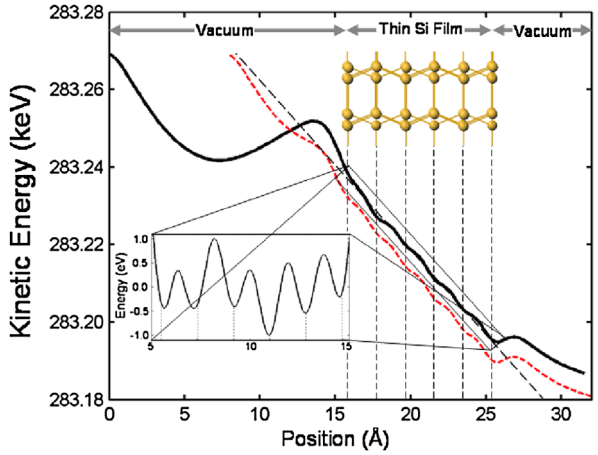

FIG. 3 (color online). The kinetic energy (KE) of a Mg ion channeling through a thin film of silicon. The dashed line is a fit to the portion of the KE of the ion while in the film. The SP is the slope of the fit. The inset is the difference between the KE and the fit. The red dashed curve corresponds to a projectile starting 8 Å from the surface of the thin film.

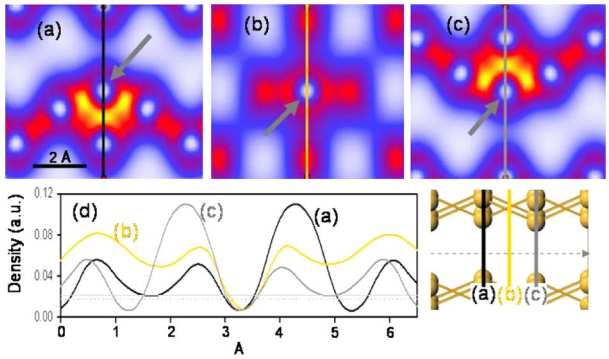

FIG. 4 (color online). Valence electron density in ⟨110⟩ planes perpendicular to the ion motion as the projectile moves through a ⟨110⟩ channel. The densities in these different planes are shown in (a), (b), and (c). (d) The line plots of the density along the vertical lines in panels (a), (b), and (c). Gray arrows point to the projectile.

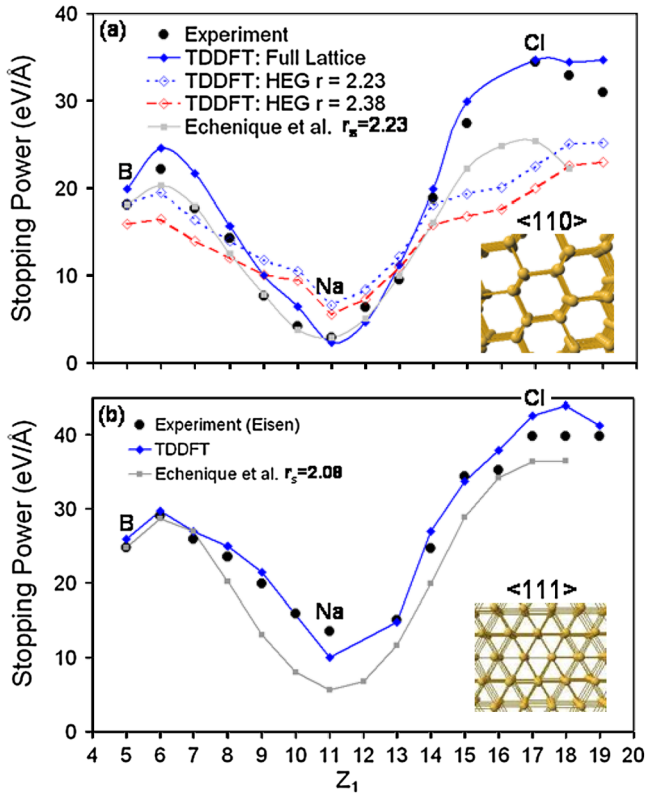

FIG. 5 (color online). SP as a function of the atomic number of the projectile atomic number Z_1 for projectiles moving through the (a) ⟨110⟩ and (b) ⟨111⟩ channels. Results are shown for experiment [6], the present TDDFT calculations ,and the results of Echenique *et al.* [15] (SP, as defined in the literature [23], has units of force).

quantitative agreement with the experimental data for all the elements.

The TDDFT/HEG results together with the full TDDFT results in a Si crystalline film demonstrate that both dynamical effects and the inhomogeneities in the electron density in the Si crystal are essential to obtain quantitative agreement with the experimental data. In Fig. 5(b) we show TDDFT SP values for ions in the ⟨111⟩ channel of Si. Once more, there is a marked improvement in the agreement with the data. The dynamical effects and the density inhomogeneities are still substantial, but their combined effect is somewhat smaller than it is in the ⟨110⟩ channels.

As a final general note, we find that the TDDFT method described above accurately characterizes the interaction of ions and electrons without restricting the electrons to the adiabatic (BO) surface. The method is, therefore, a powerful tool for modeling systems where the nonadiabatic behavior of the electrons is crucial to the phenomenon of interest. Moreover, this approach allows one to include important dynamical effects directly in a parameter-free way.

This work was supported by the DOE CMSN, AFOSR MURI Grant No. FA9550-05-1-0306, and the McMinn Endowment at Vanderbilt University. The calculations were carried out at Vanderbilt University's ACCRE. We acknowledge helpful discussions with L. C. Feldman and R. A. Weller.

[1] T. L. Ferrell and R. H. Ritchie, Phys. Rev. B **16**, 115 (1977).
[2] H. Bethe, Ann. Phys. (Leipzig) **397**, 325 (1930).
[3] F. Bloch, Ann. Phys. (Leipzig) **408**, 285 (1933).
[4] J. H. Ormrod, J. R. Macdonald, and H. E. Duckworth, Can. J. Phys. **43**, 275 (1965).
[5] L. Eriksson *et al.*, Phys. Rev. **161**, 219 (1967).
[6] F. H. Eisen, Can. J. Phys. **46**, 561 (1968).
[7] J. Bøttiger and F. Bason, Radiat. Eff. **2**, 105 (1969).
[8] P. Sigmund, *Stopping of Heavy Ions: A Theoretical Approach* (Springer, Berlin, 2004), Chap. 8.
[9] J. Lindhard, K. Dan. Vidensk. Selsk. Mat. Fys. Medd. **28**, 1 (1954).
[10] J. Lindhard and M. Scharff, Phys. Rev. **124**, 128 (1961).
[11] J. Lindhard, M. Scharff, and H. E. Schiøtt, K. Dan. Vidensk. Selsk. Mat. Fys. Medd. **33**, 1 (1963).
[12] V. U. Nazarov, J. M. Pitarke, C. S. Kim, and Y. Takada, J. Phys. Condens. Matter **16**, 8621 (2004).
[13] V. U. Nazarov, J. M. Pitarke, C. S. Kim, and Y. Takada, Phys. Rev. B **71**, 121106(R) (2005).
[14] J. S. Briggs and A. P. Pathak, J. Phys. C **6**, L153 (1973).
[15] P. M. Echenique, R. M. Nieminen, J. C. Ashley, and R. H. Ritchie, Phys. Rev. A **33**, 897 (1986).
[16] V. H. Kumar and A. P. Pathak, J. Phys. Condens. Matter **5**, 3163 (1993).
[17] M. Penalba, A. Arnau, and P. M. Echenique, Nucl. Instrum. Methods Phys. Res., Sect. B **67**, 66 (1992).
[18] E. Runge and E. K. U. Gross, Phys. Rev. Lett. **52**, 997 (1984).
[19] A. Zangwill and P. Soven, Phys. Rev. Lett. **45**, 204 (1980).
[20] H. Tal-Ezer and R. Kosloff, J. Chem. Phys. **81**, 3967 (1984).
[21] J. Theilhaber, Phys. Rev. B **46**, 12990 (1992).
[22] See http://dft.sandia.gov/socorro.
[23] Stopping power, defined as the energy loss per unit path length, has units of force. However, by convention it is referred to as power.